Multifunctional polymeric micelles loaded with doxorubicin and poly(dithienyl-diketopyrrolopyrrole) for near-infrared light-controlled chemo-phototherapy of cancer cells

Hui Liu[a,#], Kai Wang[a], Cangjie Yang[a], Shuo Huang[a], Mingfeng Wang[a,*]

[a] School of Chemical and Biomedical Engineering, Nanyang Technological University, 62 Nanyang Drive, Singapore 637459.

*To whom correspondence should be addressed. E-mail: mfwang@ntu.edu.sg

Electronic Supplementary Information (ESI) available: [details of more characterization data]. See DOI: 10.1039/x0xx00000x

#Present address: Institute for Clean Energy & Advanced Materials, Faculty of Materials & Energy, Southwest University, 2 Tiansheng Road, Chongqing 400715, P. R. China.

---

* To whom correspondence should be addressed. E-mail: mfwang@ntu.edu.sg

- Total number of words: 3370;
- Table: 1; Schemes: 2; Figures: 6

Abstract:

Polymeric micelles loaded with multiple therapeutic modalities are important to overcome challenges such as drug resistance and improve the therapeutic efficacy. Here we report a new polymer micellar drug carrier that integrates chemotherapy and photothermal therapy in a single platform. Specifically, a narrow bandgap poly(dithienyl-diketopyrrolopyrrole) (PDPP) polymer was encapsulated together with a model anticancer drug doxorubicin (DOX) in the hydrophobic cores of polymeric micelles formed by Pluronic F127, an amphiphilic poly(ethylene oxide)-poly(propylene oxide)-poly(ethylene oxide) triblock copolymer. The PDPP polymer served as an organic photothermal agent that absorbs near-infrared light (700-1000 nm) and transforms into heat efficiently. The dual functional micelles co-loaded with PDPP and DOX in the hydrophobic compartment showed good colloidal stability after being stored at 4 ^{o}C at least over two months, and remained visibly stable after 808-nm laser irradiation. The loaded DOX had negligible effect on the size and photothermal property of the micelles. The release of DOX from the micelles could be enhanced by the "breathing" effect of shrinking/swelling of the micelles induced by the temperature change, owing to the thermosensitive nature of the F127 polymers. Importantly, the ternary F127/PDPP/DOX micelles under 808-nm laser irradiation showed enhanced cytotoxicity against cancer cells such as *HeLa* cells, compared to F127 micelles containing single modality of either PDPP or DOX only.

Keywords: Polymeric micelles, Temperature-change dependent property, Drug controlled release, Chemotherapy, Photothermal therapy

1. Introduction

Cancer still remains one of the most life-threatening diseases to human beings worldwide, despite the development of a myriad of drug delivery systems (including nanomedicines) towards cancer treatment over decades of research and significant investment.[1-5] Among a variety of approaches for cancer therapy, photothermal therapy (PTT) has shown its advantages of high selectivity and minimal invasiveness in treatment of cancers.[4, 6] This method takes advantage of the near-infrared (NIR) light (700-1100 nm) that shows less invasiveness and deep tissue-penetration because of the minimal adsorption of hemoglobin and water molecules in this spectral window.[7, 8] Till now, the developed NIR photothermal agents mainly focus on two categories, inorganic and organic. Inorganic NIR absorbers with desirable performance have been extensively developed, including but not limited to gold-based nanomaterials,[9-13] carbon-based nanostructures,[14-17] copper chalcogenide semiconductors,[18-21] and transition-metal-based nanostructures.[22-26] However, their high PTT efficacy may be compromised by the potential toxicity and poor biodegradability of these inorganic nanomaterials, which may be difficult to be excreted and retain in the body for a long period.[27, 28]

NIR phototermal agents based on organic molecules[29, 30] and polymers[31-33] have emerged as promising alternatives to inorganic counterparts. Several kinds of polymers such as polyaniline,[34] polypyrrole,[35] and polydopamine[4] have been explored to be PTT agents for tumor treatment applications. However, these conducting polymers with poor solubility and processibility often result in nanoparticles that are difficult to control their sizes, shapes, and optical properties. Here, we report a narrow bandgap semiconducting polymer poly(dithienyl-diketopyrrolopyrrole) (PDPP) with improved solubility in organic solvents and more defined chemical structure, molecular weight as well as optical properties for efficient PTT treatment of cancer cells.

Besides PTT, chemotherapy involving anti-cancer drugs remains one of the most widely used approach for clinical treatment of cancers. The intrinsic hydrophobic property of many anti-cancer drugs limits their applications in cancer therapy. Many kinds of drug delivery systems have been developed to

overcome this limitation.[36-39] Furthermore, many attempts have been taken to combine PTT and chemotherapy in order to achieve an enhanced cancer-killing effect,[10, 25, 40-43],[44] but the PTT agents previously involved were mainly limited to inorganic materials such as heavy-metal nanoparticles with aforementioned issues of long-term degradability and toxicity.

In the present work, we employed a narrow-bandgap hydrophobic polymer PDPP as a NIR photothermal agent which shows strong absorption of light in the region of near-infrared wavelength. PDPP, which serves as an organic photothermal agent[45] expected with improved biocompatibility and biodegradability compared to inorganic counterparts, was encapsulated into the core of micelles formed by Pluronic 127 (F127). F127 is a commercially available amphiphilic triblock polymer composed of poly(ethylene oxide)-*b*-poly(propylene oxide)-*b*-poly(ethylene oxide) [PEO-PPO-PEO] that self-assembles into micelles with a hydrophobic core and hydrophilic corona in aqueous solution when the concentration is above the critical micelle concentration (CMC).[29, 46-48] The particle size and morphology of the formed micelles as well as their stability were characterized. In order to enhance the therapeutic effect against cancer, the formed micelles were employed as drug delivery carries to load doxorubicin (DOX) as an anti-cancer drug. The dual-functional micelles co-loaded with PDPP and DOX showed controllable release of DOX upon temperature change or NIR light irradiation, resulting in enhanced therapeutic effect against cancer cells compared to the micelles with either PDPP or DOX.

2. Experimental Section

2.1. Materials

Pluronic® F127 and thiazolyl blue tetrazolium bromide (MTT) were obtained from Sigma. Tetrahydrofuran (THF) and triethylamine (TEA) were purchased from Sigma-Aldrich. All these chemicals were used as received. Doxorubicin hydrochloride (DOX·HCl) was obtained from Beijing HuaFeng United Technology CO. Ltd (Beijing, China). Water used in all experiments was purified using a Milli-Q POD water purification system (Millipore, Bedford, MA) with resistivity higher than 18.2 MΩ.cm. Synthetic and characterization details of PDPP polymers are presented in Supporting

Information.

2.2. Preparation of F127/PDPP micelles

In a typical preparation process, F127/PDPP micelles were formed using the solvent evaporation method as following. Firstly, F127 and PDPP were separately dissolved in THF overnight. Then, F127 (100 mg/mL) in THF and PDPP (4 mg/mL) in THF were mixed together by vortex with the weight ratio of F127/PDPP at 20/1. An aliquot of the well-mixed solution (0.27 mL) was injected into 1.2 mL of water under stirring. After 3 mins, the mixture was kept in an open vial in a fume hood overnight. After evaporation of the THF, F127/PDPP micelles can be formed in aqueous solution.

Blank F127 micelles were also formed as control using the similar method. 0.12 mL of F127 solution (THF, 100 mg/mL) was was injected into 1.2 mL of water under stirring. After 3 mins, the mixture was kept in an open vial in a fume hood overnight. After evaporation of the THF, blank F127 micelles can be formed in aqueous solution.

2.3. Loading of DOX using the formed F127/PDPP micelles

Neutralized DOX was loaded into the hydrophobic core of the F127/PDPP composite micelles through the following process. Firstly, 0.17 mL of doxorubicin hydrochloride solution (2 mg/mL in water) was added into 0.6 mL of F127/PDPP aqueous solution (F127, 5 mg/mL) under stirring. After 5 min, TEA with 5 molar equivalents of DOX was added into the mixture slowly. The mixture was stirred overnight to completely neutralize the acid to allow the compartmentalization of DOX into the hydrophobic part of the micelles. After stirred overnight, the mixture was collected and centrifuged at 6000 rpm for 5 min to remove the unloaded DOX precipitate. The precipitate was collected and re-dissolved in 0.1 M HCl, and further measured the absorbance at 490 nm to calculate the encapsulation efficiency and loading content of F127/PDPP micelles.

F127/DOX micelles as control in the absence of PDPP were prepared using a method similar to what is described above.

2.4. Characterization techniques

^{1}H-NMR spectrum was recorded on a Bruker Avance II 300 MHz spectrometer in $C_2D_2Cl_4$ at 100 ^{o}C. The morphology of the formed micelles was characterized using transmission electron microscope (TEM) (CarlZeiss Libar 120 Plus). Their hydrodynamic diameters at different temperatures and surface Zeta-potentials were measured using dynamic light scattering (DLS) (BI-200SM, Brookhaven, USA). UV-Vis-NIR spectra of the micelles before and after DOX-loading were record on a UV-Vis-NIR spectrophotometer (Varian Cary 5000 spectrophotometer).

The stability of the formed F127/PDPP micelles was also investigated. After being stored at room temperature for different time periods, their hydrodynamic diameters were measured. The drug-loading content and encapsulation efficiency of the micelles were determined using a UV-Vis spectrophotometer (SHIMADZU UV-2450).

2.5. Photothermal evaluation

The formed dispersion of F127/PDPP micelles was diluted with water, resulting in the PDPP concentration at 40, 20, 10 and 5 ppm, respectively. 1.5 mL of the solution at each concentration was used to evaluate the photothermal effect under irradiation of a 808-nm laser with a power density of 1.0 W/cm^2. Each sample was irradiated for 10 min and allowed to cool down for the next 10 min, which was counted as one cycle. Pure water without micelles was also tested as control. The reproducibility of the temperature evaluation was investigated by 5 cycles of heating-cooling process.

The stability of the micelles after laser irradiation was studied after 4 h treatment under an 808-nm laser with a power density of 1.0 W/cm^2. After the laser treatment, the TEM image, UV-Vis-NIR spectra and hydrodynamic diameter of the samples were measured.

2.6. In vitro DOX release from F127/PDPP micelles and blank F127 micelles

The release assay of DOX from micelles was performed in pH 7.4 PBS buffer at 37 ^{o}C-water bath

for 24 h. The samples were packed in a dialysis bag, which was placed in a vial containing PBS buffer. At each predetermined time interval, 2 mL of the buffer was taken out and the same volume of fresh buffer was replenished to keep the whole volume constant. The buffers taken out were measured by UV-Vis spectrophotometer to determine the drug-loading content and encapsulation efficiency. The DOX release upon temperature change was studied by using laser treatment and cooling at room temperature (RT-treatment group). At each predetermined time interval, the sample in the dialysis bag was subjected to laser treatment for 10 min (45 ^{o}C) or cooling down at room temperature (25 ^{o}C) over the same period, after which the sample was sent back into the 37 ^{o}C water bath. The DOX release was also performed under different thermostatic conditions at 25 and 45 ^{o}C, respectively. For each group, the measurements were carried out in triplicate.

2.7. In vitro cytotoxicity assay

HeLa cells (a human cervical carcinoma cell line) were purchased from ATCC and cultured using MEM medium supplemented with 10 % fetal bovine serum and 1 % penicillin-streptomycin at 37 ^{o}C and 5 % CO_2.

An MTT colorimetric assay was used to quantify the viability of cells treated with F127/PDPP, F127/PDPP-DOX, F127 and F127/DOX micelles at different concentrations. Firstly, the cytotoxicity of micelles before DOX-loading was measured. Briefly, 1.5×10^4 HeLa cells per well were seeded into a 96-well plate. After overnight incubation to bring the cells to confluence, the medium was replaced with fresh medium containing the above micelles with PDPP concentrations between 0 and 15 ppm. Blank F127 micelles with an equivalent F127 concentration were also tested as control. After 24 h incubation, the medium were removed and each well was washed using PBS buffer twice. Then MTT in PBS solution (5 mg/mL) was added and the cells were incubated for additional 4 h under normal culture conditions. The assays were carried out according to the manufacturer's instructions and the absorbance of each well was recorded at 570 nm using a microplate reader (Tecan, Infinite 200, Austria). For each sample, mean and standard deviation for the triplicate wells were reported.

To study the PTT effect on the cell viability, 1.5×10^4 HeLa cells in 96-well plate were incubated with F127/PDPP with PDPP concentration of 5, 10, 15 ppm, respectively, for 12 h. Then the media containing F127/PDPP were removed and each well was washed with PBS buffer twice. The treated cells were irradiated by an 808 nm laser at a power density of 1.0 W/cm^2 for 10 min. A standard MTT assay stated above was used to measure the cell viability.

To study the effect of DOX and the combined effect of PTT and DOX, 1.5×10^4 HeLa cells in 96-well plate were incubated with F127/PDPP-DOX and F127-DOX micelles with PDPP concentration of 5, 10, 15 ppm, respectively, for 12 h. Then the media containing micelles were removed and each well was washed with PBS buffer twice. For laser treatment group, the treated cells were irradiated by an 808-nm laser at a power density of 1.0 W/cm^2 for 10 min. A standard MTT assay stated above was used to measure the cell viability.

3. Results and Discussion

3.1. Micelle preparation and characterization

A narrow bandgap polymer PDPP (M_n = 21600 g/mol, M_w/M_n = 3.3) was synthesized via direct arylation polymerization[49] and employed here as a NIR-light absorber to transform NIR light into heat. Its ^{1}H-NMR spectrum can be found in Figure S1. The UV-Vis-NIR absorption spectrum (Figure 1a) of PDPP polymer in THF shows their strong absorption around 800 nm. The micelles were prepared in the presence of F127 triblock polymer using a method of nanoprecipitation[50-52], followed by evaporation of THF (Scheme 1). Aqueous solution of doxorubicin hydrochloride (DOX•HCl) was added into the solution of the micelles and TEA was added to neutralize the acid, resulting in partition of the DOX into the hydrophobic compartment of the F127/PDPP micelles.

The UV-Vis-NIR absorption spectra of F127/PDPP micelles before and after loading of DOX can be found in Figure 1b. It is noticed that the absorption peak has blue-shifted from 887 to 816 nm after formation of micelles as compared to the spectrum of pure PDPP polymer. This may be caused by the

change in the physical conformation of the polymer chains when packed together in micelles[53] After loading DOX, the absorption around 500 nm increased obviously due to the absorption of DOX. From DLS data, the size of the micelles remained similar after loading of DOX (Figure 1d) as compared to the original F127/PDPP micelles (Figure 1c). The diameters of the micelles before and after loading of DOX were both around 50 nm. This was further confirmed by the TEM images (Figure S2a and S2b), from which no obvious difference in size could be observed. The surface potentials of F127/PDPP and F127 micelles before and after loading DOX were kept similar (Table S1). The prepared F127/PDPP micelles were quite stable when their aqueous solutions stored at 4 ºC for at least two months (Figure S3). The DLS results suggested neither noticeable change in particle size nor any significant particle aggregation. Meanwhile blank F127 micelles of similar size without PDPP were also formed as control and used to load DOX. The blank micelles showed no absorption around 800 nm (Figure S4a), making them suitable as control. From DLS (Figure S4b) and TEM (Figure S4d) data, blank F127 micelles displayed a size similar to that of F127/PDPP micelles. However, after DOX loading, the size of F127-DOX micelles increased obviously in aqueous solution (Figure S4c) as observed with DLS, which is consistent with the TEM images shown in Figure S4e.

In order to investigate the photothermal properties, F127/PDPP micelles with different concentrations were treated with an 808-nm laser at a power density of 1.0 W/cm^2. With the increase in PDPP concentration from 5 to 40 ppm, the final temperature of the solution could reach up to 45 ºC by laser irradiation (808 nm, 1.0 W/cm^2) for 10 min (Figure 2a). The increase of temperature can reach up to 20 ºC when PDPP concentration was 40 ppm (Figure 2b). The temperature curve could be repeated with good consistency (Figure 2c). The loaded DOX and F127 parts have no influence on the temperature curve (Figure 2d) due to their negligible absorption in the NIR region. The F127/PDPP micelles were subjected to laser treatment for 4 h to investigate their photothermal stability. The temperature increased with the laser irradiation and reached a plateau at 50 ºC (Figure S5a). After laser treatment, there was no obvious change in their UV-Vis-NIR absorption spectra (Figure S5b). The DLS

and TEM results (Figure S5c and S5d) also showed that the size and morphology of the micelles remained similar to those of the original micelles without laser treatment. All of these data proved that the formed F127/PDPP micelles showed desirable photothermal stability.

3.2. In vitro release of DOX from micelles

The DOX encapsulation efficiency and loading content of F127/PDPP micelles as a kind of drug carrier were measured according to the calibration curve of the light absorption of DOX at 490 nm (Figure S6). The encapsulation efficiency and loading content of F127/PDPP micelles were calculated to be around 54.1% and 3.3%, respectively (Table 1). Blank F127 micelles showed DOX-loading capacity similar to that of F127/PDPP micelles. From the DOX release profile at 37 ºC (Figure 3a), it can be seen that around 30% of DOX released from the F127/PDPP micelles in 24 h. F127/DOX micelles showed a faster release than F127/(PDPP+DOX) micelles, which may be due to the enhanced hydrophobic interaction between PDPP and DOX in the core of F127 micelles.

The release of DOX could be enhanced by laser treatment. Under 808-nm laser irradiation, the release of DOX from F127/PDPP micelles increased from 33.3% to 55.1% at 24 h, nearly 1.7 times compared to the group without laser treatment (Figure 3b). Surprisingly, this laser-enhanced DOX release phenomenon was also found in F127/DOX micelles without PDPP, which was even much more effective than from F127/PDPP/DOX micelles (Figure 3c).

In order to understand this non-expected phenomenon of enhanced release of DOX from blank F127 micelles, which showed almost no NIR absorption and transformation ability described above, another RT-treatment control was conducted. For F127/PDPP RT-treatment group, it can be seen that RT treatment could also enhance the release of DOX, which is even more effective than laser treatment (Figure 4a). For blank F127 RT-treatment group, RT treatment could enhance the DOX release at similar degree with the laser treatment (Figure 4b). So it is believed that it was the temperature change (i.e. from 37 ºC to room temperature during 808-nm laser irradiation of F127/DOX micelles) that

enhanced the release of DOX as shown in Scheme 2 and Scheme S1. Because of the block architecture and lower critical solution temperature (LCST) of PEO and PPO, aqueous solution of Pluronic micelle exhibits temperature sensitivity.[48] When temperature increases, the hydrophobicity of the PPO and PEO segments of F127 polymers increases and the core of the micelles tends to shrink,[29, 47, 48] leading to the repulsion of water out of the core as well as molecular DOX. When temperature decreases, an opposite phenomenon appears, leading to the absorption of water as well as DOX into the core of the micelles. This could make RT-treatment more effective in enhancing DOX release than laser treatment, especially for F127/PDPP/DOX micelles. The different effects of temperature-change for F127/PDPP and F127 micelles may be caused by their different hydrophobic core and structures. The role played by temperature-change was further proven by the release of DOX from F127/PDPP micelles under thermostatic conditions (Figure 4c). It is clear that the release of DOX remained similar regardless of the temperature.

To prove the hypothesis of the photothermal induced phase transition of F127 micelles, the change in micelles diameters was further investigated by DLS measurements (Figure 5). It is proved that the size of the micelles deceased with the increase in temperature from 25 to 45 ºC.[48, 54] Meanwhile, the size change of blank F127 micelles was more remarkable than that of F127/PDPP micelles, which led to the faster release of DOX from F127/DOX micelles.

3.3. In vitro cell study

For biomedical applications, it is important to ensure that the materials have desirable biocompatibility. Firstly, the cytocompatibility of the formed micelles was tested against HeLa cells (Figure 6a). It can be seen that the formed micelles displayed good cytocompatibility in the PDPP concentration range of 0.5 to 15 ppm after 24 h incubation with HeLa cells (Figure 6a). With the laser treatment, the cell viability decreased with significant difference compared with the no-laser treatment group (Figure 6b). When cells were treated with DOX-loaded micelles, the cell viability decreased

dramatically (Figure 6c), indicating the effectiveness of DOX in killing cancer cells. It is also noted that F127-DOX micelles can cause more cell death than F127/PDPP-DOX micelles, which further proved that DOX was released more quickly from F127 micelles.

The combination of PTT and chemotherapeutic effect of DOX is expected to enhance the anticancer effect. As shown in Figure 6d, MTT results displayed that either chemotherapy (DOX) or PTT alone could not achieve ideal therapeutic results against tumor cells. However, by combining these two approaches together, cell viability decreased to 4.8% at a PDPP concentration of 15 ppm, which was better than either laser treatment (cell viability was 61.8%) or DOX treatment (cell viability was 15.3%) separately.

4. Conclusion

In summary, we have presented a multifunctional tertiary polymeric micelle consisting of both narrow bandgap PDPP polymers as NIR photothermal agents and DOX as anti-cancer drugs in the hydrophobic compartment of F127 micelles. The resulting micelles showed synergistic photo-chemo therapeutic effect against cancer cells. The formed micelles were stable and could be used to load anti-cancer drugs such as DOX. The photothermal property of the micelles depended on the laser irradiation time and PDPP concentration, while the loaded DOX had negligible effect on the size and photothermal property of the micelles. The size of the micelles decreased with the increase of temperature, which was proven by the DLS data. Furthermore, the release of DOX from the micelles could be enhanced the "breathing" effect of shrinking/swelling of the micelles induced by repeating temperature change, owing to the temperature-sensitivity of the F127 polymers. MTT results showed that the micelles without loading of DOX displayed desirable cytocompatibility in the dark. After incubating cells with F127/PDPP micelles, laser treatment decreased cell viability significantly. Furthermore, a combination of the photothermal therapy (PDPP under laser treatment) and chemotherapy (DOX) using the F127/PDPP/DOX tertiary micelles induced cytotoxicity up to 95% against HeLa cells under 808-nm laser irradiation. These results demonstrated that enhanced anticancer effect could be achieved by

combining PTT and chemotherapy, which is promising for further animal studies and clinical trials.

Acknowledgments

M.W. is grateful to the funding support by a start-up grant (M4080992.120) of Nanyang Assistant Professorship from Nanyang Technological University, and AcRF Tier 2 (ARC 36/13) from the Ministry of Education, Singapore. We thank Dr. L. H. Nguyen for help in the cytotoxicity measurement and Dr. S. Y. Chew for valuable feedback on this work.

References

[1] D. Yoo, J.-H. Lee, T.-H. Shin, J. Cheon, Theranostic magnetic nanoparticles, Acc. Chem. Res., 44 (2011) 863-874.
[2] R. Bardhan, S. Lal, A. Joshi, N.J. Halas, Theranostic nanoshells: From probe design to imaging and treatment of cancer, Acc. Chem. Res., 44 (2011) 936-946.
[3] Q. Chen, H.T. Ke, Z.F. Dai, Z. Liu, Nanoscale theranostics for physical stimulus-responsive cancer therapies, Biomaterials, 73 (2015) 214-230.
[4] Y. Liu, K. Ai, J. Liu, M. Deng, Y. He, L. Lu, Dopamine-melanin colloidal nanospheres: An efficient near-infrared photothermal therapeutic agent for in vivo cancer therapy, Adv. Mater., 25 (2013) 1353-1359.
[5] V.J. Venditto, F.C. Szoka, Cancer nanomedicines: So many papers and so few drugs!, Adv Drug Deliver Rev, 65 (2013) 80-88.
[6] S. Lal, S.E. Clare, N.J. Halas, Nanoshell-enabled photothermal cancer therapy: impending clinical impact, Acc. Chem. Res., 41 (2008) 1842-1851.
[7] M. Chen, X. Fang, S. Tang, N. Zheng, Polypyrrole nanoparticles for high-performance in vivo near-infrared photothermal cancer therapy, Chem. Commun., 48 (2012) 8934-8936.
[8] N.W.S. Kam, M. O'Connell, J.A. Wisdom, H.J. Dai, Carbon nanotubes as multifunctional biological transporters and near-infrared agents for selective cancer cell destruction, Proc. Natl. Acad. Sci. U. S. A., 102 (2005) 11600-11605.
[9] Y. Tian, S. Shen, J. Feng, X. Jiang, W. Yang, Mussel-inspired gold hollow superparticles for photothermal therapy, Adv. Healthc. Mater., 4 (2015) 1009-1014.
[10] H. Deng, F. Dai, G. Ma, X. Zhang, Theranostic gold nanomicelles made from biocompatible comb-like polymers for thermochemotherapy and multifunctional imaging with rapid clearance, Adv. Mater., 27 (2015) 3645-3653.
[11] Y. Zeng, D. Zhang, M. Wu, Y. Liu, X. Zhang, L. Li, Z. Li, X. Han, X. Wei, X. Liu, Lipid-AuNPs@PDA nanohybrid for MRI/CT imaging and photothermal therapy of hepatocellular carcinoma, ACS Appl. Mater. Inter., 6 (2014) 14266-14277.
[12] R.K. Kannadorai, G.G.Y. Chiew, K.Q. Luo, Q. Liu, Dual functions of gold nanorods as photothermal agent and autofluorescence enhancer to track cell death during plasmonic photothermal therapy, Cancer Lett., 357 (2015) 152-159.
[13] L. Dykman, N. Khlebtsov, Gold nanoparticles in biomedical applications: Recent advances and perspectives, Chem. Soc. Rev., 41 (2012) 2256-2282.
[14] Z. Hu, F. Zhao, Y. Wang, Y. Huang, L. Chen, N. Li, J. Li, Z. Li, G. Yi, Facile fabrication of a C60-

polydopamine-graphene nanohybrid for single light induced photothermal and photodynamic therapy, Chem. Commun., 50 (2014) 10815-10818.
[15] K. Yang, L. Feng, X. Shi, Z. Liu, Nano-graphene in biomedicine: Theranostic applications, Chem. Soc. Rev., 42 (2013) 530-547.
[16] C. Li, S. Bolisetty, K. Chaitanya, J. Adamcik, R. Mezzenga, Tunable carbon nanotube/protein core-shell nanoparticles with NIR-and enzymatic-responsive cytotoxicity, Adv. Mater., 25 (2013) 1010-1015.
[17] J. Shi, L. Wang, J. Zhang, R. Ma, J. Gao, Y. Liu, C. Zhang, Z. Zhang, A tumor-targeting near-infrared laser-triggered drug delivery system based on GO@Ag nanoparticles for chemo-photothermal therapy and X-ray imaging, Biomaterials, 35 (2014) 5847-5861.
[18] Q. Tian, M. Tang, Y. Sun, R. Zou, Z. Chen, M. Zhu, S. Yang, J. Wang, J. Wang, J. Hu, Hydrophilic flower-like CuS superstructures as an efficient 980 nm laser-driven photothermal agent for ablation of cancer cells, Adv. Mater., 23 (2011) 3542-3547.
[19] Q. Tian, F. Jiang, R. Zou, Q. Liu, Z. Chen, M. Zhu, S. Yang, J. Wang, J. Wang, J. Hu, Hydrophilic Cu9S5 nanocrystals: A photothermal agent with a 25.7% heat conversion efficiency for photothermal ablation of cancer cells in vivo, ACS Nano, 5 (2011) 9761-9771.
[20] Q. Tian, J. Hu, Y. Zhu, R. Zou, Z. Chen, S. Yang, R. Li, Q. Su, Y. Han, X. Liu, Sub-10 nm Fe3O4@Cu2-xS core-shell nanoparticles for dual-modal imaging and photothermal therapy, J. Am. Chem. Soc., 135 (2013) 8571-8577.
[21] C.M. Hessel, V.P. Pattani, M. Rasch, M.G. Panthani, B. Koo, J.W. Tunnell, B.A. Korgel, Copper selenide nanocrystals for photothermal therapy, Nano Lett., 11 (2011) 2560-2566.
[22] Z. Chen, Q. Wang, H. Wang, L. Zhang, G. Song, L. Song, J. Hu, H. Wang, J. Liu, M. Zhu, Ultrathin PEGylated W18O49 nanowires as a new 980 nm-laser-driven photothermal agent for efficient ablation of cancer cells in vivo, Adv. Mater., 25 (2013) 2095-2100.
[23] L. Cheng, J. Liu, X. Gu, H. Gong, X. Shi, T. Liu, C. Wang, X. Wang, G. Liu, H. Xing, PEGylated WS2 nanosheets as a multifunctional theranostic agent for in vivo dual-modal CT/photoacoustic imaging guided photothermal therapy, Adv. Mater., 26 (2014) 1886-1893.
[24] S.S. Chou, B. Kaehr, J. Kim, B.M. Foley, M. De, P.E. Hopkins, J. Huang, C.J. Brinker, V.P. Dravid, Chemically exfoliated MoS2 as near-infrared photothermal agents, Angew. Chem. Int. Edit., 125 (2013) 4254-4258.
[25] T. Liu, C. Wang, X. Gu, H. Gong, L. Cheng, X. Shi, L. Feng, B. Sun, Z. Liu, Drug delivery with PEGylated MoS2 nano-sheets for combined photothermal and chemotherapy of cancer, Adv. Mater., 26 (2014) 3433-3440.
[26] W. Yin, L. Yan, J. Yu, G. Tian, L. Zhou, X. Zheng, X. Zhang, Y. Yong, J. Li, Z. Gu, High-throughput synthesis of single-layer MoS2 nanosheets as a near-infrared photothermal-triggered drug delivery for effective cancer therapy, ACS Nano, 8 (2014) 6922-6933.
[27] S. Sharifi, S. Behzadi, S. Laurent, M.L. Forrest, P. Stroeve, M. Mahmoudi, Toxicity of nanomaterials, Chem. Soc. Rev., 41 (2012) 2323-2343.
[28] J. Li, X. Chang, X. Chen, Z. Gu, F. Zhao, Z. Chai, Y. Zhao, Toxicity of inorganic nanomaterials in biomedical imaging, Biotechnol. Adv., 32 (2014) 727-743.
[29] S. Huang, R.K. Kannadorai, Y. Chen, Q. Liu, M. Wang, A narrow-bandgap benzobisthiadiazole derivative with high near-infrared photothermal conversion efficiency and robust photostability for cancer therapy, Chem. Commun., 51 (2015) 4223-4226.
[30] S. Huang, U.P. Kumar, H. Liu, M. Pramanik, M. Wang, A dual-functional benzobisthiadiazole derivative as an effective theranostic agent for near-infrared photoacoustic imaging and photothermal therapy, J Mater. Chem. B, 4 (2016) 190-196.
[31] X. Song, Q. Chen, Z. Liu, Recent advances in the development of organic photothermal nano-agents, Nano Res., 8 (2015) 340-354.
[32] L. Xu, L. Cheng, C. Wang, R. Peng, Z. Liu, Conjugated polymers for photothermal therapy of cancer, Polym. Chem., 5 (2014) 1573-1580.
[33] X. Wang, J. Zhang, Y. Wang, C. Wang, J. Xiao, Q. Zhang, Y. Cheng, Multi-responsive photothermal-chemotherapy with drug-loaded melanin-like nanoparticles for synergetic tumor ablation,

Biomaterials, 81 (2016) 114-124.
[34] J. Zhou, Z. Lu, X. Zhu, X. Wang, Y. Liao, Z. Ma, F. Li, NIR photothermal therapy using polyaniline nanoparticles, Biomaterials, 34 (2013) 9584-9592.
[35] Z. Zha, X. Yue, Q. Ren, Z. Dai, Uniform polypyrrole nanoparticles with high photothermal conversion efficiency for photothermal ablation of cancer cells, Adv. Mater., 25 (2013) 777-782.
[36] Z. Xu, S. Liu, Y. Kang, M. Wang, Glutathione- and pH-responsive nonporous silica prodrug nanoparticles for controlled release and cancer therapy, Nanoscale, 7 (2015) 5859-5868.
[37] J. Zhu, L. Zheng, S. Wen, Y. Tang, M. Shen, G. Zhang, X. Shi, Targeted cancer theranostics using alpha-tocopheryl succinate-conjugated multifunctional dendrimer-entrapped gold nanoparticles, Biomaterials, 35 (2014) 7635-7646.
[38] S. Wen, H. Liu, H. Cai, M. Shen, X. Shi, Targeted and pH-responsive delivery of doxorubicin to cancer cells using multifunctional dendrimer-modified multi-walled carbon nanotubes, Adv. Healthc. Mater., 2 (2013) 1267-1276.
[39] Y. Wang, R. Guo, X. Cao, M. Shen, X. Shi, Encapsulation of 2-methoxyestradiol within multifunctional poly(amidoamine) dendrimers for targeted cancer therapy, Biomaterials, 32 (2011) 3322-3329.
[40] Y. Liu, J. Bai, X. Jia, X. Jiang, Z. Guo, Fabrication of multifunctional SiO2@GN-serum composites for chemo-photothermal synergistic therapy, ACS Appl. Mater. Inter., 7 (2015) 112-121.
[41] L. Wu, M. Wu, Y. Zeng, D. Zhang, A. Zheng, X. Liu, J. Liu, Multifunctional PEG modified DOX loaded mesoporous silica nanoparticle@CuS nanohybrids as photo-thermal agent and thermal-triggered drug release vehicle for hepatocellular carcinoma treatment, Nanotechnology, 26 (2015) 025102.
[42] A. Agarwal, M.A. Mackey, M.A. El-Sayed, R.V. Bellamkonda, Remote triggered release of doxorubicin in tumors by synergistic application of thermosensitive liposomes and gold nanorods, ACS Nano, 5 (2011) 4919-4926.
[43] G. Tian, X. Zhang, X. Zheng, W. Yin, L. Ruan, X. Liu, L. Zhou, L. Yan, S. Li, Z. Gu, Y. Zhao, Multifunctional RbxWO3 nanorods for simultaneous combined chemo-photothermal therapy and photoacoustic/CT imaging, Small, (2014) 4160-4170.
[44] L. Cheng, C. Wang, L.Z. Feng, K. Yang, Z. Liu, Functional Nanomaterials for Phototherapies of Cancer, Chem Rev, 114 (2014) 10869-10939.
[45] Y.J. Wu, K. Wang, S. Huang, C. Yang, M. Wang, Near-infrared light-responsive semiconductor polymer composite hydrogels: Toward spatial/temporal controlled release via photothermal “sponge” effect, ACS Appl. Mater. Interfaces, 9 (2017) 13602-13610.
[46] C. Allen, D. Maysinger, A. Eisenberg, Nano-engineering block copolymer aggregates for drug delivery, Colloid. Surface. B, 16 (1999) 3-27.
[47] Q. Zhou, X. Guo, T. Chen, Z. Zhang, S. Shao, C. Luo, J. Li, S. Zhou, Target-specific cellular uptake of folate-decorated biodegradable polymer micelles, J. Phys. Chem. B, 115 (2011) 12662-12670.
[48] Y. Chen, X. Li, Near-infrared fluorescent nanocapsules with reversible response to thermal/pH modulation for optical imaging, Biomacromolecules, 12 (2011) 4367-4372.
[49] K. Wang, M. Wang, Hyperbranched narrow‐bandgap DPP homopolymers synthesized via direct arylation polycondensation, J. Poly. Sci. Part A: Poly. Chem., 55 (2017) 1040-1047.
[50] M. Wang, S. Kumar, A. Lee, N. Felorzabihi, L. Shen, F. Zhao, P. Froimowicz, G.D. Scholes, M.A. Winnik, Nanoscale co-organization of quantum dots and conjugated polymers using polymeric micelles as templates, J. Am. Chem. Soc., 130 (2008) 9481-9491.
[51] S. Huang, S. Liu, K. Wang, C. Yang, Y. Luo, Y. Zhang, B. Cao, Y. Kang, M. Wang, Highly fluorescent and bioresorbable polymeric nanoparticles with enhanced photostability for cell imaging, Nanoscale, 7 (2015) 889-895.
[52] C. Yang, H. Liu, Y. Zhang, Z. Xu, X. Wang, B. Cao, M. Wang, Hydrophobic-Sheath Segregated Macromolecular Fluorophores: Colloidal Nanoparticles of Polycaprolactone-Grafted Conjugated Polymers with Bright Far-Red/Near-Infrared Emission for Biological Imaging, Biomacromolecules, 17 (2016) 1673-1683.

[53] B.J. Schwartz, Conjugated polymers as molecular materials: How chain conformation and film morphology influence energy transfer and interchain interactions, Annu. Rev. Phys. Chem., 54 (2003) 141-172.
[54] Z. Zeng, Z. Peng, L. Chen, Y. Chen, Facile fabrication of thermally responsive Pluronic F127-based nanocapsules for controlled release of doxorubicin hydrochloride, Colloid Polym. Sci., 292 (2014) 1521-1530.

Table 1. Data of DOX loading for micelles.

Micelles	Encapsulation efficiency (%)	Loading content (%)
F127/PDPP	54.1 ± 4.9	3.3 ± 0.3
F127	56.5 ± 3.4	3.6 ± 0.2

Figure caption

Scheme 1. Schematic illustration of the preparation of F127/PDPP/DOX tertiary micelles via the solvent evaparation method.

Scheme 2. Schematic illustration of the size change ("breathing" effect of shrinking/swelling) of F127/PDPP micelles induced by the change of the temperature.

Figure 1. (a) UV-Vis-NIR absorption spectrum of PDPP polymers dissolved in THF. (b) UV-Vis-NIR absorption spectra of F127/PDPP micelles and DOX-loaded F127/PDPP micelles. Inset is the corresponding photo of the micelles solution. DLS data for F127/PDPP (c) and F127/PDPP-DOX (d) micelles.

Figure 2. (a) Temperature curves of F127/PDPP micelles solution with different PDPP concentrations under 808 nm laser irradiation at a power density of 1.0 W/cm^2. (b) Temperature increase of F127/PDPP micelles solution with different PDPP concentrations under same laser treatment. (c) Five cycles of temperature increase curve with PDPP concentration at 40 ppm under same laser treatment. (d) Temperature curve of the micelles before and after loading of DOX. Pure water was used as control for all experiments.

Figure 3. (a) Release profiles of DOX from F127/PDPP and F127 micelles at 37 ºC in pH 7.4 PBS buffer. (b) Laser-triggered release of DOX from F127/PDPP micelles, the samples were irradiated with an 808 nm laser (1.0 W/cm^2) for 10 min at time point of 1, 3, 6, 9, 12 h. (c) Release of DOX from F127 micelles, the samples were treated with the same procedure of laser irradiation as in Figure (b). Except the laser irradiation process which was conducted in air under ambient conditions, all the release processes underwent in a thermostatic water bath at 37 ºC. In other words, the samples shown in Figure (b) and (c) without laser irradiation (black square) were maintained at 37 ºC during the whole release process, whereas the sample (F127/DOX micelles) with laser irradiation (red dot) in Figure (c) experienced multicycles of back-and-forth temperature change from 37 to 25 ºC. In contrast, the

temperature change in the sample (F127/PDPP/DOX micelles) with laser irradiation in Figure (b) is expected to be less significant compared to the sample (F127/DOX micelles) shown in Figure (c) due to the photothermal effect of PDPP in the former. The enhanced release of DOX shown in the sample (F127/DOX micelles) with laser irradiation (red dot) in Figure (c) may be attributed to the repeating swelling-shrinking of the micelles (Scheme 2) associated with the back-and-forth temperature change from 37 to 25 ºC.

Figure 4. (a) Release profile of DOX from F127/PDPP micelles at 37 ºC in pH 7.4 PBS buffer. At time point of 1, 3, 6, 9, and 12 h, the sample was irradiated with an 808 nm laser (1.0 W/cm^2) (labled as 45 ºC) or just left at room temperature (labled as 25 ºC) for 10 min. (b) Release profile of DOX from F127 micelles under water bath of 37 ºC with the same treatment. (c) Release profile of DOX from F127/PDPP micelles under different temperature conditions.

Figure 5. DLS data for F127/PDPP (a) and F127 (b) micelles under different temperature conditions. (c) DLS diameter histograms for F127/PDPP and F127 micelles under different temperature conditions.

Figure 6. (a) Cell viability of HeLa cells treated with a series of F127-based micelles for 24 h measured by MTT assay. (b) Cell viability of HeLa cells treated with F127/PDPP micelles for 12 h, then the cells were irradiated using an 808 nm laser (1.0 W/cm2) for 10 min. (c) Cell viability of HeLa cells treated with DOX-loaded micelles for 12 h. (d) Cell viability of HeLa cells treated with micelles for 12 h, then the cells were irradiated using an 808 nm laser (1.0 W/cm2) for 10 min. All labled concentration refers to PDPP concentration of F127/PDPP micelles. The blank F127 group and pure DOX group used an equivalent F127 and DOX concentration to the F127/PDPP-DOX group. Statistical significance was calculated using the ANOVA method and is indicated with (*) for $p < 0.05$ and (***) for $p < 0.0001$.

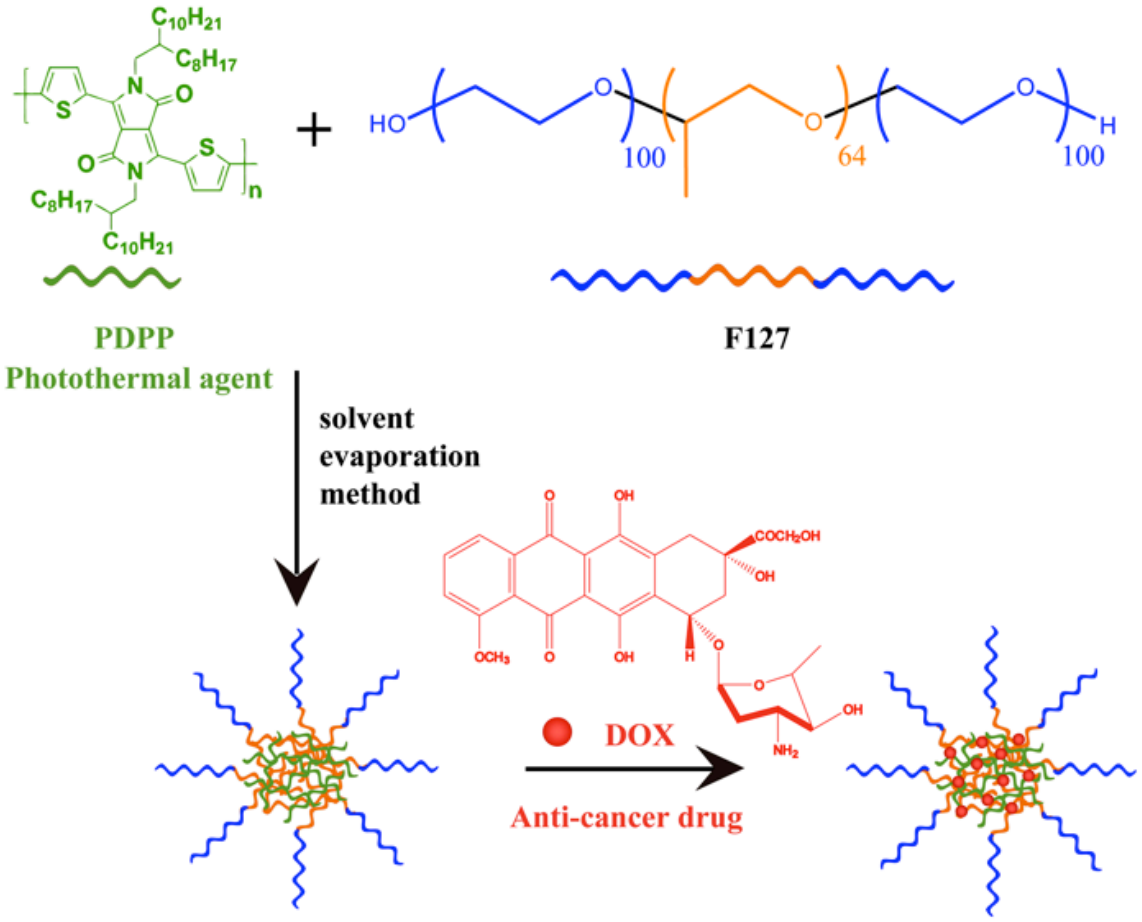

Scheme 1
Liu et al.

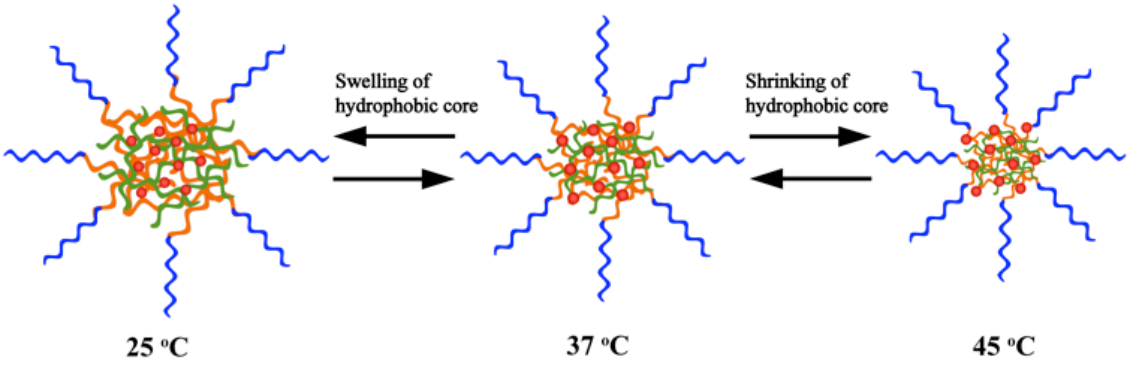

Scheme 2
Liu et al.

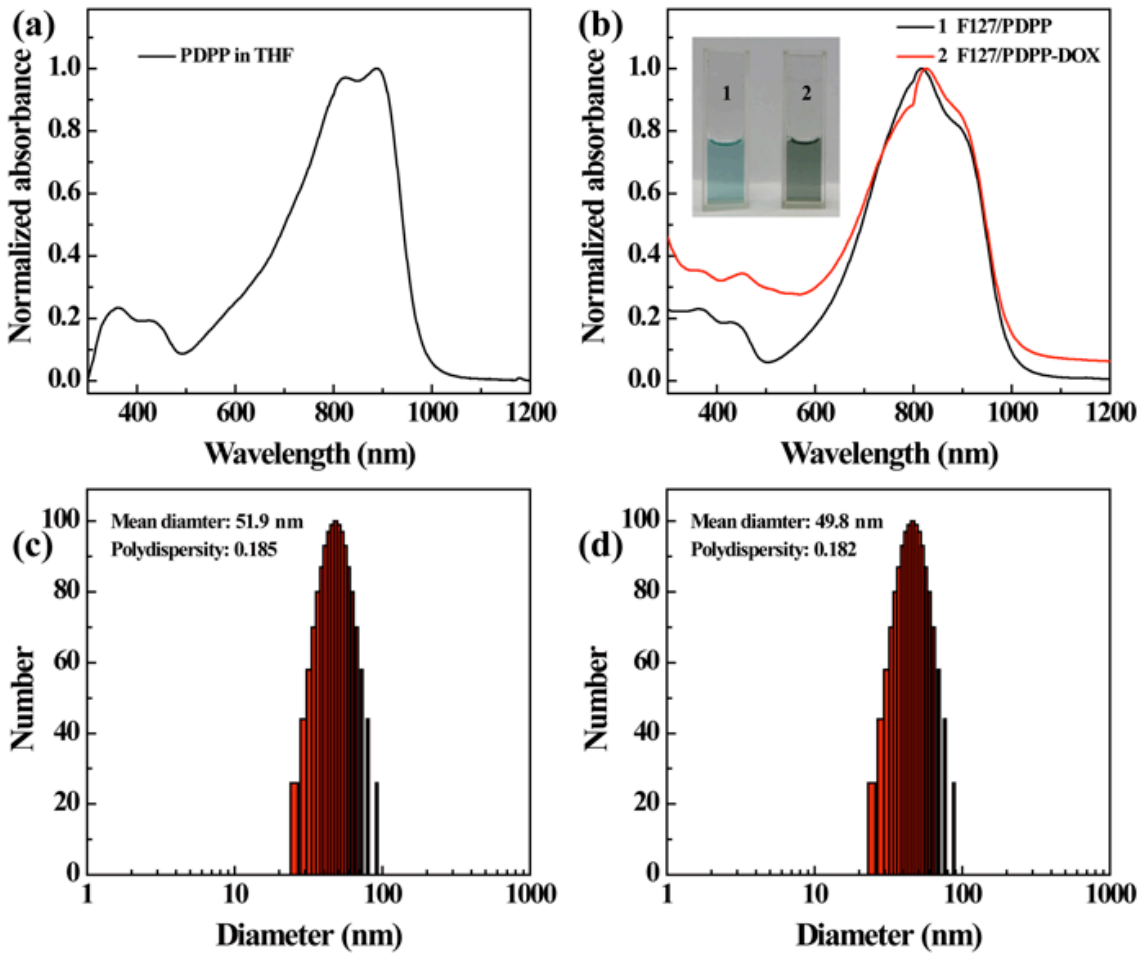

Figure 1
Liu et al.

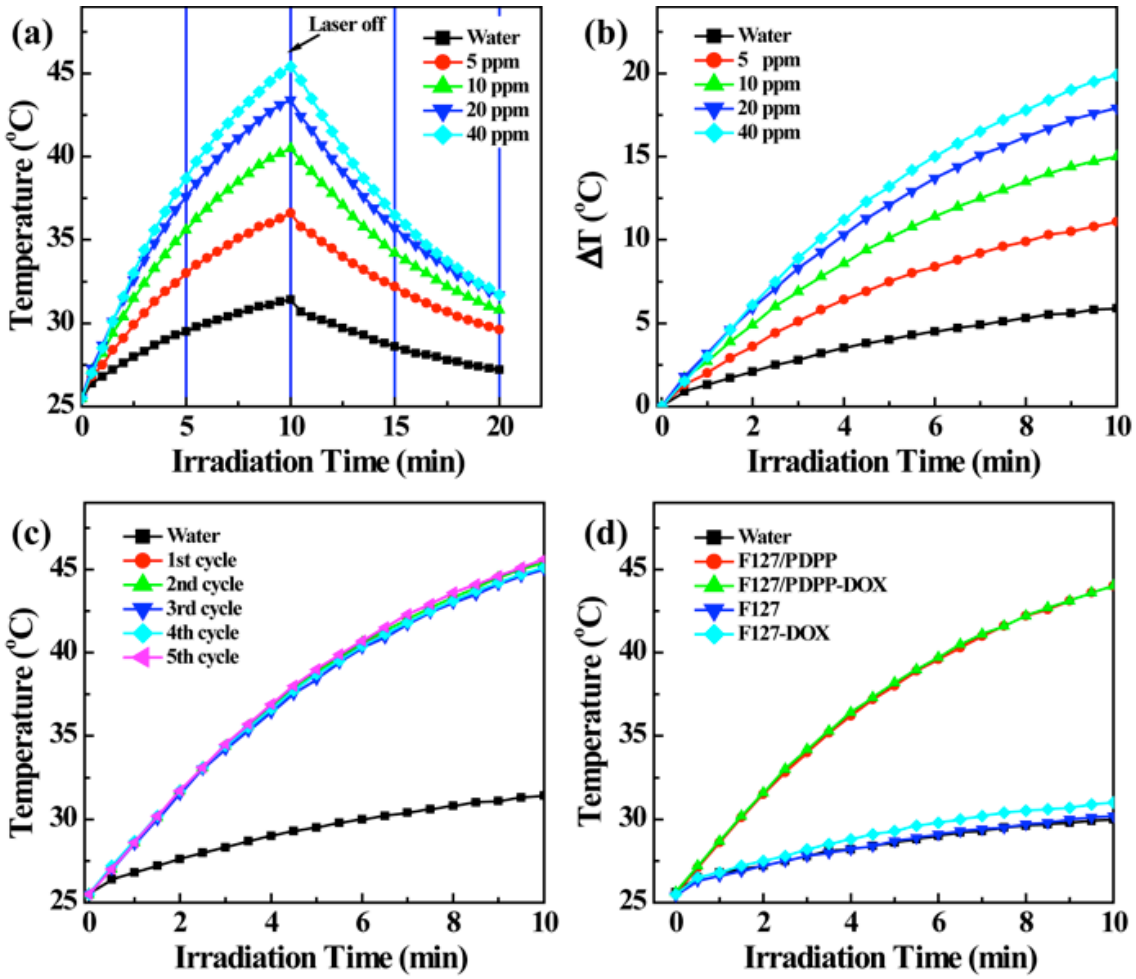

Figure 2
Liu et al.

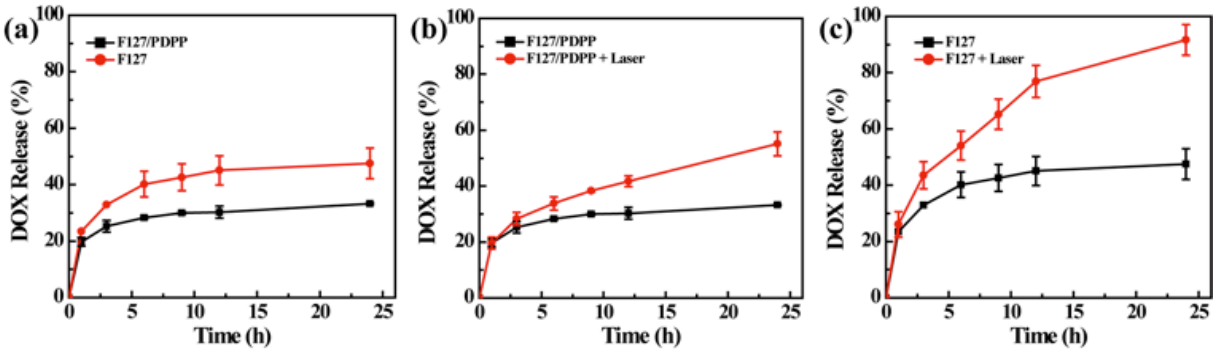

Figure 3
Liu et al.

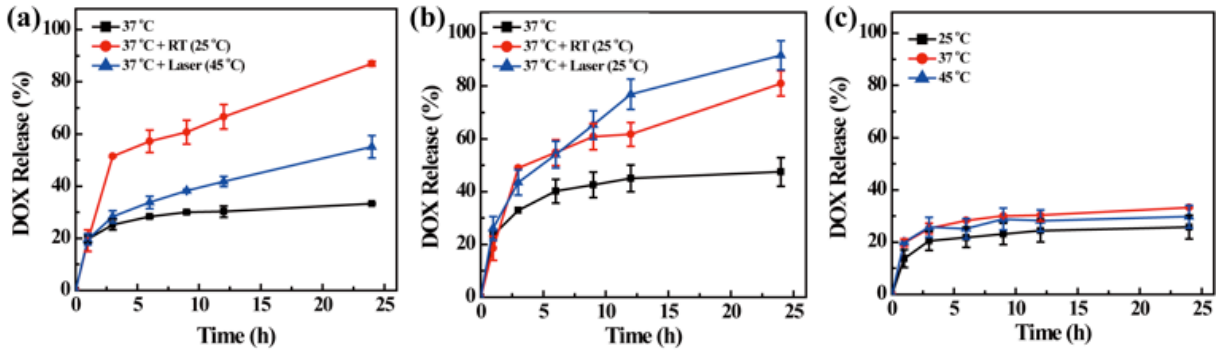

Figure 4
Liu et al.

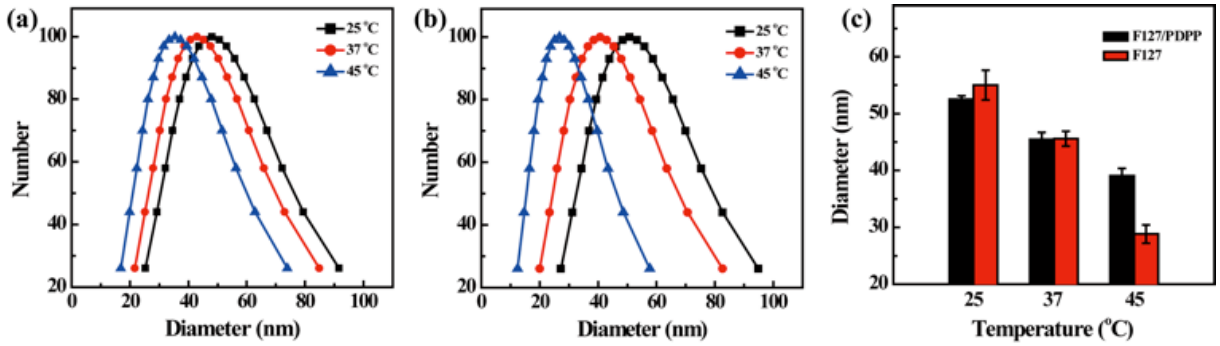

Figure 5
Liu et al.

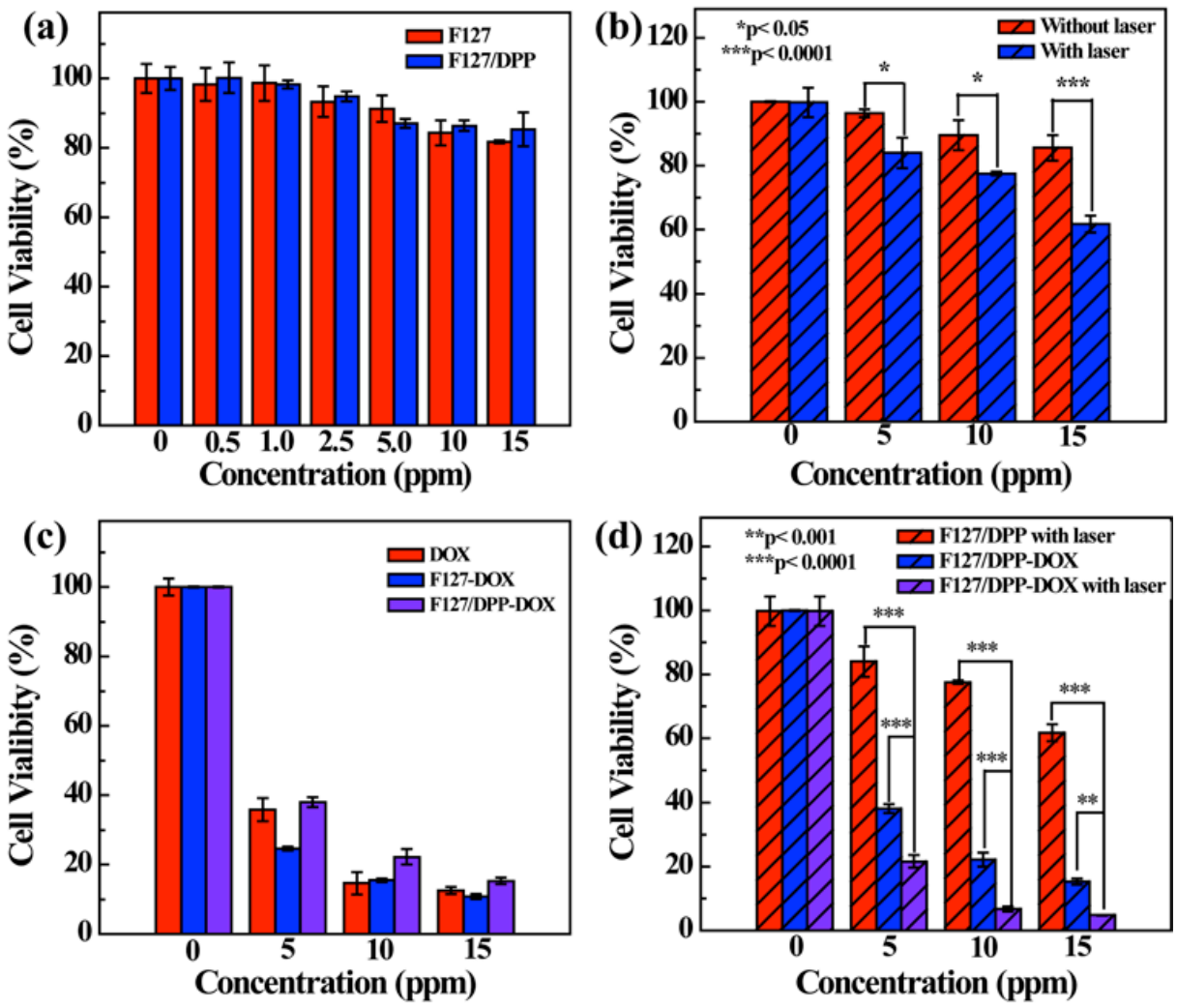

Figure 6
Liu et al.